Seasonal variations of high-latitude field-aligned currents inferred from Ørsted and Magsat observations

F. Christiansen, V. O. Papitashvili,[1] and T. Neubert[2]

Solar-Terrestrial Physics Division, Danish Meteorological Institute, Copenhagen, Denmark

Received 21 July 2000; revised 25 June 2001; accepted 27 June 2001; published 20 February 2002.

[1] In this paper we report on field-aligned currents inferred from high-precision three-component geomagnetic field observations made on board the Danish satellite Ørsted over polar regions. Because of a slow drift in local time of the satellite orbit through the "noon-midnight" sector, we were able to study the seasonal dependence of the dynamic properties of the dayside and nightside field-aligned current systems over the Northern and Southern Hemispheres. We find an average over-the-pole distance between dayside and nightside currents of 32° during summer but 37° during winter and 36° during equinox. The decrease in the size of the summer polar cap is caused by a shift of both daytime and nighttime current systems to higher magnetic latitudes. For comparison, the dawn-dusk cross-polar distance of the Region 1/Region 2 field-aligned currents has been determined from high-precision data observed by Magsat, a satellite flown in 1979–1980 in a "dawn-dusk" orbit. The latter results show that the dawn-dusk distance between R1/R2 currents exhibits little seasonal dependence and amounts to ~34° for all seasons in both polar caps. The seasonal dependence is confirmed for the high-latitude field-aligned intensities; they are larger by a factor of 1.5–1.8 in the sunlit (summer) polar cap in comparison with the winter hemisphere. Our results suggest that the R1/R2 and dayside field-aligned currents are well balanced between the pairs of downward/upward currents for all seasons as well as between hemispheres during equinox. We were not able to confirm results reported in earlier studies that the net currents tend to increase with an enhancement of ionospheric conductivity caused by the solar illumination or substorm activity. *INDEX TERMS:* 2708 Magnetospheric Physics: Current systems (2409); 2409 Ionosphere: Current systems (2708); 2736 Magnetospheric Physics: Magnetosphere/ionosphere interactions; 2776 Magnetospheric Physics: Polar cap phenomena; *KEYWORDS:* Field-aligned currents, magnetosphere, ionosphere, polar cap, seasonal dependence

1. Introduction

[2] Average distributions of field-aligned currents (FACs) over the polar regions have been the subject of numerous studies since their first outline as the Region 1/Region 2 (R1/R2) current system derived from TRIAD satellite observations [*Zmuda and Armstrong*, 1974; *Iijima and Potemra*, 1976]. This R1/R2 organization of the currents is very persistent in the dawn and dusk sectors of magnetic local time (MLT), whereas the currents near noon are known to depend strongly on the interplanetary magnetic field conditions [for example, see *Iijima et al.*, 1984; *Potemra et al.*, 1984; *Erlandson et al.*, 1988]. Validity of the sheet current approximation to the field-aligned currents has been examined by *Hoffman et al.* [1994] and *Yamamoto et al.* [2000]. *Watanabe et al.* [1998] have investigated field-aligned currents in the magnetospheric ground state, and *Hoffman et al.* [1994] have investigated field-aligned currents associated with auroral substorms in the nighttime sector. The active role of the ionospheric conductivity on the magnetosphere-ionosphere coupling has recently been investigated extensively from the viewpoints of aurora occurrence [e.g., *Newell et al.*, 1998] and strong field-aligned electric fields in the downward FAC region [e.g., *Carlson et al.*, 1998; *Elphic et al.*, 1998]. However, the seasonal dependence of the field-aligned currents was examined only by *Fujii et al.* [1981], who showed that the dayside currents in the summer were located at 1°–3° higher latitude than during winter.

[3] The first Danish satellite, Ørsted, was launched on February 23, 1999, into a low-Earth, polar orbit with inclination 96.48°, perigee 649 km, and apogee 865 km; the satellite has been in operation for ~3 years. The ascending node was at 1411 LT at launch, and the orbit plane drifts −0.9 min local time per day. One of the primary objectives of the mission is to survey the Earth's magnetic field with the highest possible accuracy in order to study the main geomagnetic field and its secular variation. Thus the satellite carries a three-axial magnetometer and other instrumentation for high-precision, absolute measurements of the field (better than 5 nT per component) [*Neubert et al.*, 2001]. During the first year of operation, data were processed for quiet magnetic conditions to determine a 13th-order spherical harmonics model and an IGRF-2000 model truncated to 10th order [*Olsen et al.*, 2000a]. The follow-on Ørsted Initial Field Model was derived to the 19th order [*Olsen et al.*, 2000b].

[4] In this paper we study the seasonal dependence of the high-latitude FAC systems, particularly their spatial distribution, using high-precision magnetic field observations from the Ørsted and Magsat satellites. We have chosen Ørsted observations obtained during equinox (August 25 to October 11, 1999) and northern winter (November 26, 1999, to January 24, 2000). The orbit's ascending node during these intervals drifted between 1145–1100 and 1020–0925 LT, respectively. However, because of the offset between geographic and geomagnetic poles, the satellite covered near-geomagnetic-pole regions in both hemispheres quite well. To complement the Ørsted observations with dawn/dusk observations,

[1] Also at Space Physics Research Laboratory, University of Michigan, Ann Arbor, Michigan, USA.

[2] Now at Danish Space Research Institute, Copenhagen, Denmark.

0148-0227/02/2001JA900104

we include an analysis of data from the Magsat mission. Two periods were selected: November 26 to January 24, 1979 (northern winter) and February 10 to April 9, 1980 (equinox). The main goal of this study is to obtain the average locations of the field-aligned currents depending on the season for the dawn-dusk (Magsat) and dayside-nightside (Ørsted) MLT sectors.

2. Method

[5] The Ørsted Science Data Center (http://www.dmi.dk/projects/oersted/) delivers the satellite magnetic field measurements in an Earth-centered geographic coordinate system. The magnetic field disturbances over the polar regions were obtained by subtracting the IGRF-2000 model from the three-component magnetic field measurements (1 s resolution). The magnetic field disturbance vectors were then transformed into the corrected geomagnetic (CGM) coordinate system defined by the same main field model [e.g., *Gustafsson et al.*, 1992]. The location of the satellite is given as the altitude adjusted CGM latitude and MLT hour; that is, the CGM coordinates used in this paper are taken at the Earth's surface at the magnetic field-line footprint of the satellite's position. Magnetic east is defined as the direction of constant CGM latitude, magnetic north is perpendicular to this direction, and magnetic local time is obtained as an hour angle from the subsolar point.

[6] The geomagnetic field lines are nearly vertical over the polar region. For example, according to the GEO-CGM code (http://nssdc.gsfc.nasa.gov/space/cgm/), the field lines whose footprints intercept 45° CGM latitude are inclined from 24° to 30° at the satellite's average altitude ~750 km. At 65° CGM their inclination varies from 9.5° to 14.5°, and at 85° CGM it varies from 1.0° to 4.5°. In this study we limit ourselves to considering the horizontal components of the residuals for the field-aligned current detection. This causes a maximum error in the δX component (i.e., almost along the satellite track in the "CGM latitude-MLT" coordinates) that will be proportional to a cosine of the inclination angle, that is, 13% for the worst case at 45° CGM (where the satellite doesn't detect any currents at all). The maximum error at 65° CGM and higher (where most of the FACs are detected) will not exceed 3%. Note that the equivalent error in the (perpendicular to the track) δY component will be even smaller.

[7] Using Ampere's law, we may calculate the field-aligned current density as the curl of the corresponding magnetic field disturbances:

$$\mu_0 j_\parallel = \frac{\partial B_y}{\partial x} - \frac{\partial B_x}{\partial y}, \tag{1}$$

where x and y are perpendicular to the magnetic field. Assuming vertical field line geometry, we may let x denote magnetic north (i.e., perpendicular to the CGM latitude) and y denote magnetic east. Obviously, we cannot calculate the curl from a single pass of the satellite. One way to overcome this is to collect many passes and consider average distributions of magnetic disturbances. Here, instead, we assume that the current systems are organized as "infinite" sheet currents along magnetic latitude such that $\partial/\partial y = 0$ [*Iijima and Potemra*, 1976]. We determine the current density in 1° intervals above ±45° latitude from a linear fit along the orbit, giving $\partial B_{\text{east}}/\partial l$, where l is the distance traveled along the orbit. With ω being the angle between the orbit and magnetic latitude, we then find

$$\mu_0 j_\parallel = \frac{1}{\sin\omega}\frac{\partial B_{\text{east}}}{\partial l} \tag{2}$$

Data are discarded if ω is below 45°, where the orbit is primarily tangential to CGM latitude and the assumed direction of the current sheets.

[8] The Magsat satellite data were processed the same way, subtracting the IGRF-1980 model [*Langel and Estes*, 1985] from the 0.5-s data series available from NASA's National Space Science Data Center (http://nssdc.gsfc.nasa.gov/space/).

[9] In Figure 1 we show the data coverage by Ørsted and Magsat obtained by this method for the periods selected. The numbers on the color bar refer to the number of measurements of the FACs in bins of 1° magnetic latitude and 20 min magnetic local time. Typically, 10–15 measurements of the magnetic field are used for each computation of the current density. The area covered is mainly determined by the diurnal variation of the geomagnetic coordinate system with respect to the orbit of the satellite and by the rejection of data when the orbit is not sufficiently close to perpendicular to the assumed east-west direction of the current sheets. For the relatively short time span of each of these periods (<2 months) the drift of Ørsted's orbit is of minor importance, though a difference due to the orbit drift is clearly seen between the two periods of Ørsted observations. Magsat did not drift in local time, and the data coverage is identical for the two selected periods.

[10] For reference, the classical picture of average distributions of field-aligned currents is shown in Figure 2 [*Iijima and Potemra*, 1976]. While Magsat sampled a relatively clear structure over the polar caps with distinctive R1/R2 currents, a more complex region is explored with Ørsted. Not only does Ørsted pass the polar caps both prenoon and postnoon, but the dayside current systems near noon are strongly dependent on the interplanetary magnetic field (IMF) conditions. In addition, Ørsted will at times observe three-sheet current systems on the nightside.

3. Data

[11] In Figure 3 we present an example of the Ørsted observations for two consecutive passes over both the northern and southern polar regions for the magnetic storm event on September 23, 1999. For each pass we show the horizontal component of the magnetic disturbance vectors (in a CGM latitude-MLT coordinate system) along with IZMEM model distributions of the field-aligned currents parameterized by the IMF strength and direction [*Papitashvili et al.*, 1994] (http://www.sprl.umich.edu/mist/). Beneath the polar plots are shown the corresponding three components of the magnetic disturbances as a function of time. In order to avoid artificial effects near the poles, we use a Cartesian coordinate system defined by the directions sunward (S_w, toward 1200 MLT), dawnward (D_w, toward 0600 MLT), and vertical (Z).

[12] The two orbits occur a few hours after the storm commencement when the *Dst* index began to increase, indicating the beginning of the recovery phase. The storm occurred exactly at equinox, so both polar regions are equally sunlit. The IMF data have been obtained from NASA's ACE spacecraft 1-min measurements propagated ballistically from the L1 point to the nominal magnetopause location at 12 Earth radii. The IMF values shown at the upper left corner are 40-min averages taken at the interval from 20 min before the satellite's magnetic field line footprint crosses ±55° entering the polar cap and to the end of the polar pass. The IMF vector is observed to be turning from southward to northward with a large negative B_y component and with a positive B_x component, indicating a "toward-the-Sun" IMF sector.

[13] The given IMF configuration was favorable for the development of a strong R1/R2 FAC system as well as for the existence of strong field-aligned cusp currents. During the first northern pass (Figure 3a, left), Ørsted detected an upward current (interpreted as the counterclockwise rotation of the magnetic disturbance vectors) at 75° CGM latitude near 1000 MLT and a somewhat weaker downward current at higher latitudes, while on the nightside it detected a downward current near 68° and an upward current at 63° near 0100 MLT. The underlying IZMEM model confirms the nighttime boundary but fails at the dayside, extending the R1

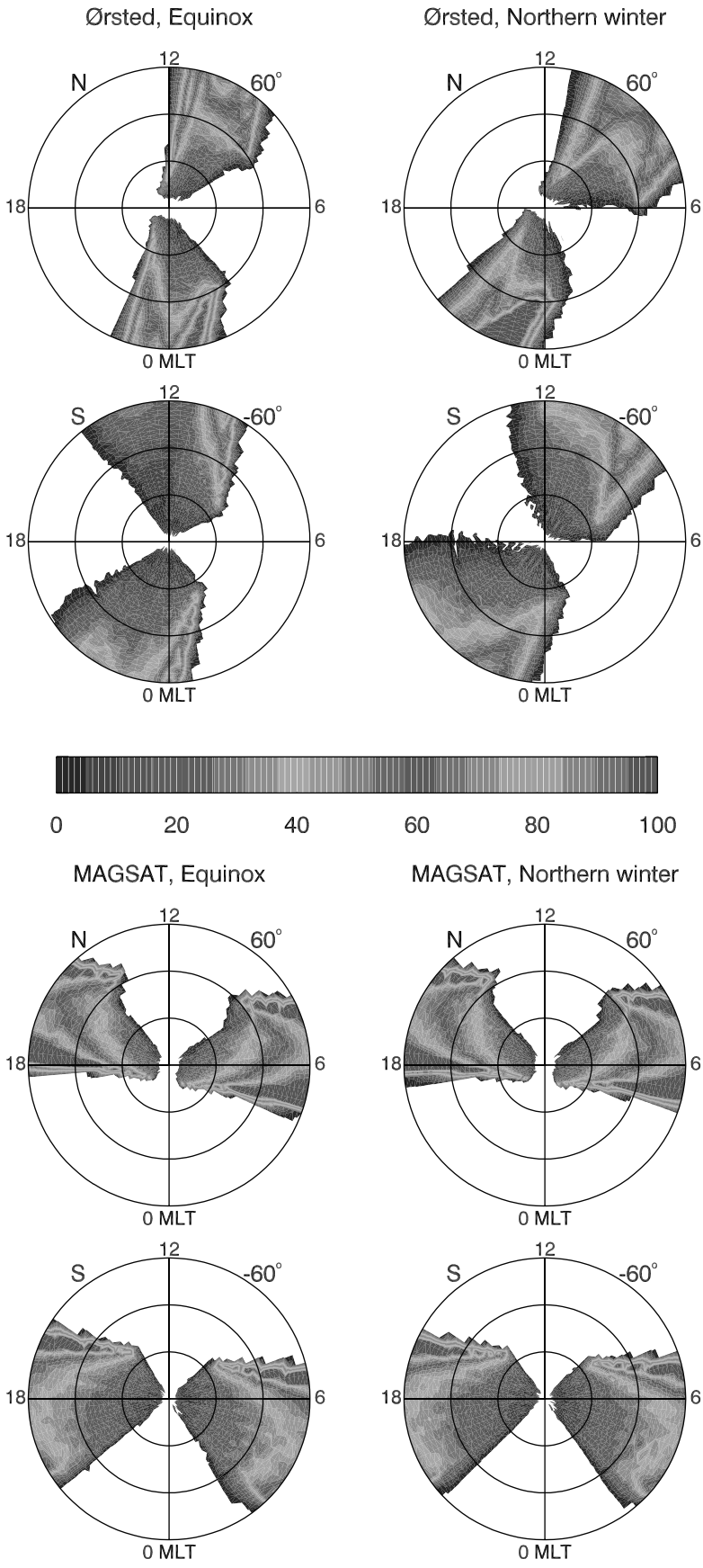
Ørsted, Equinox
Ørsted, Northern winter
N
60°
S
-60°
12
18
6
0 MLT
0
20
40
60
80
100
MAGSAT, Equinox
MAGSAT, Northern winter

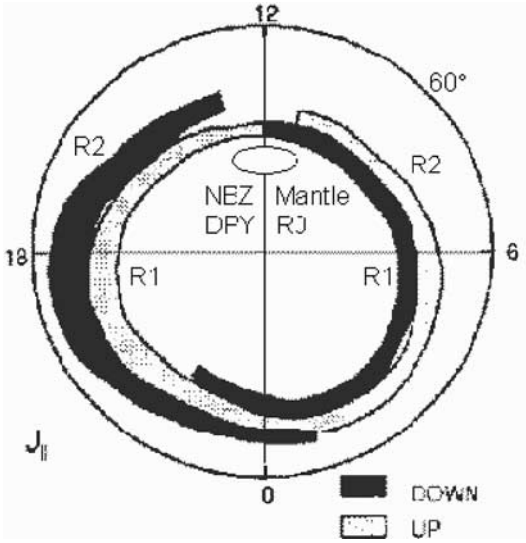

Figure 2. Average distribution of Region 1/Region 2 field-aligned currents adapted from *Iijima and Potemra* [1976]. Though it may vary strongly in position, this configuration is very persistent during various conditions (season, IMF, storms, etc.) The dayside currents poleward of Region 1 are also indicated.

downward currents to far lower latitudes than the satellite detected. On the following southern pass (Figure 3b, left), Ørsted detected a strong downward current at $-70°$ and an upward current at $-78°$ CGM latitude on the dayside and then a downward/upward pair of currents below $-70°$ on the nightside, again in best agreement with the IZMEM model on the nightside.

[14] As the IMF turned northward, the second northern pass (Figure 3a, right) shows a downward/upward pair of R1/R2 currents near 75°; the nightside R1/R2 pair breaks into small-sized FAC filaments at ~68°, manifesting themselves as oscillations in the D_w component. On the dayside of the southern polar cap we see a weak upward R2 current at $-70°$, a stronger downward R1 current at $-75°$, and a strong upward NBZ current at $-80°$. On the nightside we again see a filamentary structure rather than a clear R1/R2 separation.

[15] We note that most of the detected dayside and nightside magnetic disturbances show quasiperiodic, fine structure of the field-aligned currents, that is, the D_w component shows perturbations from multiple upward-downward minisheets (or filaments) on a background of large-scale magnetic disturbances (e.g., see last three passes in Figure 3). These variations are sometimes also seen in the S_w component, indicating that the orientation of the FAC sheets may not be exactly along magnetic latitudes. Since we are using the same binning of data (according to CGM latitude) on every orbit, such relatively fast variations are to some extent averaged out.

[16] Examples of the Magsat high-latitude field-aligned currents can be found elsewhere [e.g., *Zanetti et al.*, 1983; *Iijima and Shibaji*, 1987].

4. Results

[17] The analysis above of a few polar passes of the satellite shows that Ørsted detects the existence of both noon and midnight field-aligned currents over both polar caps. Next, we estimate the field-aligned current densities from (2) consecutively for all the orbits of the selected periods and plot the FAC densities color-coded versus CGM latitude and universal time (UT) of the orbit. We can thereby obtain the spatial distribution of both dayside and nightside current systems. Figure 4 shows the distributions of field-aligned currents inferred from the Ørsted data for equinox (left) and northern winter/southern summer (right) polar caps; red/yellow regions are downward currents, and blue regions are upward currents, while white areas generally denote a lack of available data. Note that the apparent green color that can be seen in Figure 4 is simply an effect of yellow and blue being interspersed closely and on a short distance. The shape of the area of lacking data near the poles is caused by the diurnal variation in the position of the magnetic poles (and thereby the entire magnetic coordinate system) with respect to the satellite orbit. This variation is stronger in the Southern Hemisphere since there the distance between the corrected geomagnetic and geographic poles is twice as large (16°) as in the Northern Hemisphere (8.5°). We include a plot of the northern polar cap magnetic activity index PCN (e.g., http://www.dmi.dk/projects/wdcc1/pcn/pcn.html) to indicate geomagnetically quiet (PCN < 1.5) and disturbed (PCN > 1.5) times. According to *Vassiliadis et al.* [1996], the selected PCN's division corresponds to the auroral electrojet index $AL \simeq -120$ nT.

[18] First, an obvious observation from Figure 4 is that locations of both the dayside and nightside current systems vary in time in accordance with changing geomagnetic activity. The magnetic storm on September 22–23 is clearly visible as a "spike" covering ~20° in latitude over both polar regions where FACs are detected at latitudes down to ±50°. The following days after the storm show little activity in the current systems. However, a similar significant intensification in the FAC systems occurred also during September 26–27, when a magnetic substorm developed over the polar regions; it is clearly seen over both the nightside and dayside in the Northern and Southern Hemispheres. Thus the dayside FAC systems are evidently sensitive to the substorm development at the nightside, as has been observed, for example, by *Troshichev et al.* [1997].

[19] As expected, the downward (yellow/red) and upward (blue) FACs alternate in position at the dayside; this is most likely caused by changes in the sign of the IMF B_y component. In the southern polar cap a triple-sheet FAC system (downward-upward-downward currents) is sometimes observed; its apparent variability in location fits the expected FAC configuration in accordance with the variations of the orbit plane near the premidnight sector.

[20] The results for the periods of Magsat data are shown in Figure 5. Here we also see diurnal variations caused by the position of the magnetic poles with respect to the satellite orbit. As expected, we immediately observe the existence of Region 1/Region 2 field-aligned current systems: at dawn the downward R1 currents flow at higher latitudes and the corresponding R2 upward currents flow at lower latitudes. The direction of the currents is opposite at dusk: the upward R1 currents flow at higher latitudes and the downward R2 currents flow at lower latitudes. This pair of field-aligned currents persists unchanged through varying geomagnetic activity.

[21] Although the location of the dawn-dusk FAC systems depends significantly on geomagnetic activity (see, for example, the remarkable variability of the dusk currents in the northern winter polar cap (topmost section of Figure 5, right)), the "average" locations of the current systems are fairly stable at 72°–75° CGM latitudes in both the northern and southern polar regions irrespective of the season, giving an over-the-pole distance of ~34°.

Figure 1. (opposite) Data coverage for Ørsted and Magsat in the CGM latitude-MLT coordinates. Red/yellow areas denote strong data coverage; purple/blue areas denote weak data coverage. The numbers on the color bar refer to the number of current density measurements in bins of 1° magnetic latitude and 20 min MLT. The data have been discarded where the satellites' orbits were passing the CGM latitudes at an angle below 45°. This in combination with the diurnal variation of the magnetic coordinate system relative to the satellite's orbit determines the data coverage. See color version of this figure at back of this issue.

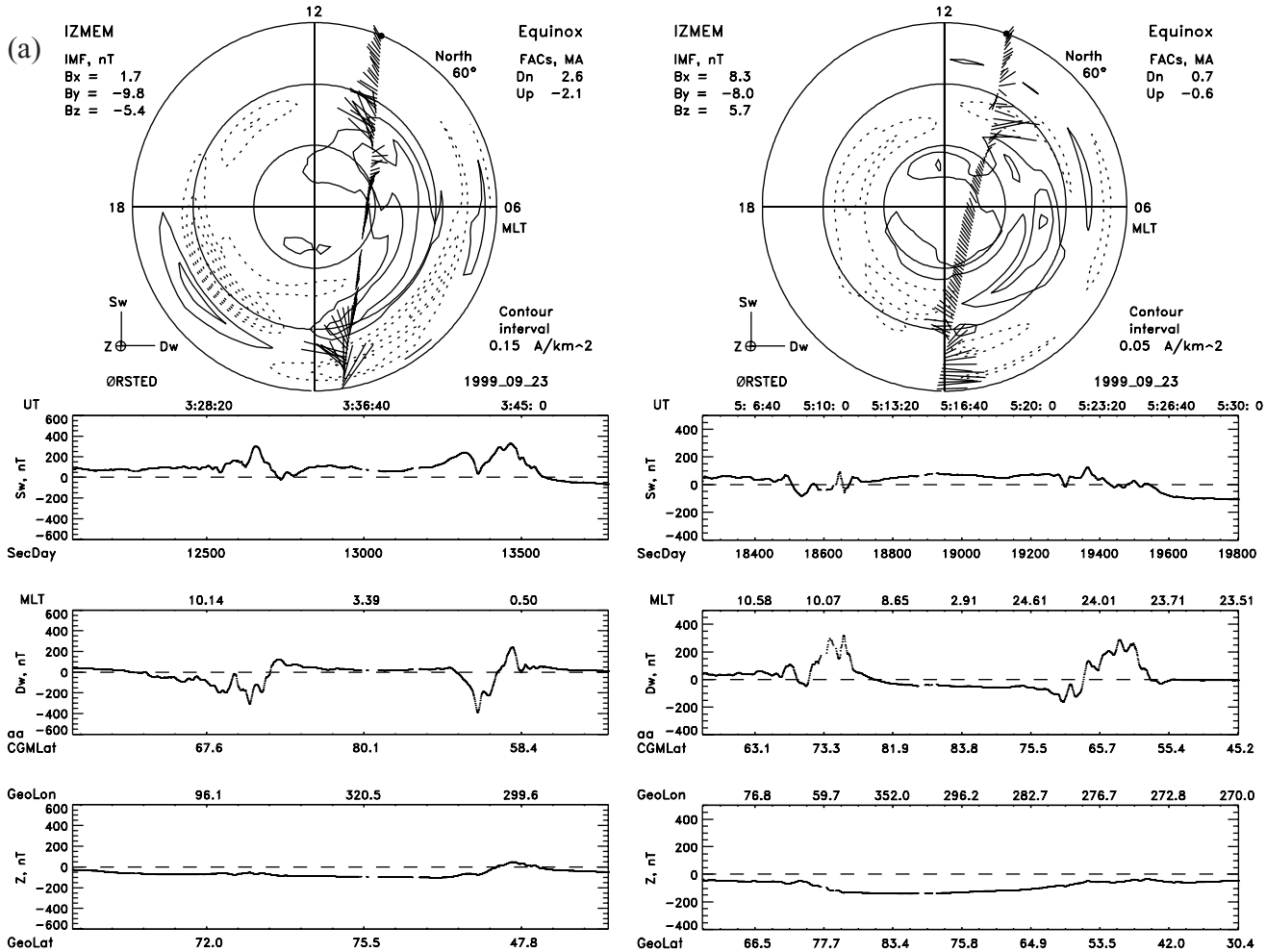

Figure 3. Two Ørsted passes over the (a) northern and (b) southern polar caps a few hours after the commencement of a magnetic storm on September 23, 1999. The dial plots show the magnetic disturbances in CGM latitude-MLT coordinates. An entry point into the polar cap is marked by a heavy dot at 60° CGM latitudes. Beneath the dial plots are shown the three components of the magnetic disturbance vectors in the coordinates S_w (sunward), D_w (dawnward), and Z (vertical). The hourly *Dst* index was −134, −133, −123, and −110 for these passes, respectively. In the dial plots are also shown IZMEM model calculations of the FACs; solid contours indicate downward current, and dashed contours indicate upward currents. The IMF conditions for each pass are printed in the top left of the dial, whereas total downward (Dn) and upward (Up) currents from the model are printed at the top right.

[22] To better analyze the field-aligned current systems shown in Figures 4 and 5, we have computed the average FAC densities versus CGM latitude for the intervals under investigation, where we have separated downward (positive) and upward (negative) currents and also separated the data in disturbed and quiet geomagnetic conditions. We compare northern winter/southern summer (solid lines) to equinox (dashed lines). The two upper plots in Figure 6 correspond to Figure 4, and the two lower plots correspond to Figure 5, with the four panels of each plot showing the average FACs of the four parts of Figures 4 and 5.

[23] With the separation of data according to the PCN index, the averages for quiet conditions are made from 424/437 Ørsted passages over the northern/southern polar caps during equinox (Figure 1, left) and 528/567 Ørsted passages over the winter/summer polar caps (Figure 1, right) the corresponding numbers of polar passages for Magsat are 726/734 for equinox (Figure 4, left) and 733/684 for winter/summer (Figure 4, right). The corresponding numbers for disturbed conditions are 139/132 and 170/167 for Ørsted and 172/172 and 174/168 for Magsat.

[24] From the data in Figure 6 we estimate the "average" location of the upward/downward FACs as well as the range in latitude where we can expect to find these currents. We also find the average strength of the FAC systems and the average total downward and upward currents. The results are summarized in Table 1 for Ørsted and in Table 2 for Magsat. Here we describe some of the features that can be seen in Figure 6 and from the Tables 1 and 2.

4.1. Location Ranges

[25] We define the FACs location range as the latitudes with an average current density of more than 0.1 $\mu A/m^2$. As expected, we find that the nightside currents are shifted to lower latitudes (by $\sim 7°$ on average) compared to the dayside currents. Compared to equinox, the currents are found at lower latitudes in the winter polar cap and at higher latitudes during summer, with the strongest effect for the dayside currents.

[26] The dawn and dusk current systems are found in considerably larger ranges than the dayside and nightside current systems, extending close to the poles. Inspection of Figure 6 reveals that the cause of this could be Region 0 currents [e.g., *Papitashvili et al.*, 2001]. For example, see the Magsat plot for quiet conditions: the

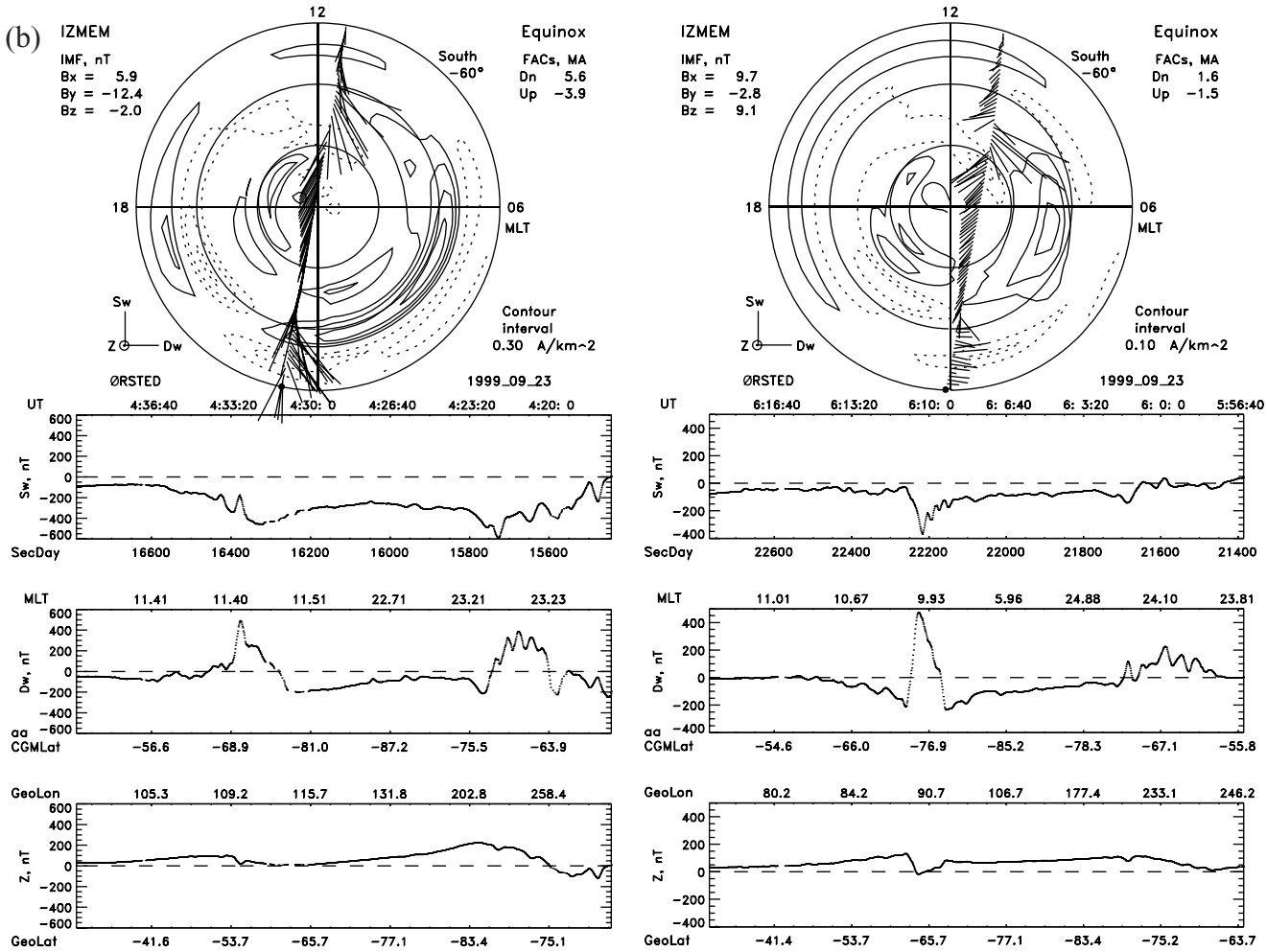

Figure 3. (continued)

R2 (R1) currents have a maximum around 70° (75°), but then significant currents are observed above 80°.

4.2. Average Positions

[27] The average positions P of the field-aligned current systems confirm the above results. While the approximate boundaries (computed from the data in Figure 5) between the "quiet" downward and upward currents at dawn and dusk are all centered near 72°–75° CGM latitude irrespective of season (67°–75° during disturbed conditions), both the "quiet" and "disturbed" dayside currents during equinox are centered at 75°–77°; the nightside currents are shifted equatorward to 66°–69°, covering a wider range of latitudes for disturbed conditions. Compared to equinox, the "quiet" currents in the summer polar cap have moved poleward by ∼3° on the dayside (from 76.0° ± 1.1° to 79.1° ± 0.8°) and by ∼2° on the nightside (from 67.9° ± 0.6° to 70.1° ± 0.4°), while during winter only the dayside currents are found to move equatorward and only by ∼1° (to 75.0° ± 0.5°) (the nightside currents are actually moving poleward by the same amount (to 68.7° ± 0.4°)), both within the statistical uncertainty of the analysis. For the "disturbed" currents the picture is less clear: during winter the "disturbed" dayside currents move equatorward by 4°–5°, while on the nightside only the upward currents show a poleward shift (by ∼3°). During summer only the dayside upward currents are shifted (equatorward by ∼2°).

[28] Averaging the upward and downward currents combined and including both quiet and disturbed conditions, we find an over-the-pole distance between the dawn and dusk field-aligned currents of 33.6° ± 1.3° for all seasons combined. This includes a slight increase in the winter polar cap caused by a strong shift equatorward of the currents during disturbed conditions. Compared to this, the over-the-pole distances between the average dayside and nightside currents are higher during equinox (36.0° ± 1.3°) and winter (37.3° ± 0.8°) and lower during summer (31.8° ± 0.9°). Note that this assessment is not statistical but rather characterizes the time intervals under investigation. More statistical studies are underway where the location and intensity of the field-aligned currents are assessed according to the IMF strength and direction.

4.3. Upward/Downward Asymmetry

[29] Comparing the relative positions of downward and upward currents in Figure 6, we see that the Ørsted data give almost identical positions for both the dayside and nightside and for all seasons. This is as expected since the average, owing to the orbit of Ørsted, is over both prenoon and postnoon observations, and the near-noon current systems are, furthermore, strongly dependent on the IMF conditions which varied during the observational periods. However, some upward/downward asymmetry is seen for the disturbed conditions in the northern winter polar cap. For this period the orbit of Ørsted has moved farther into the morning sector (see Figure 1, top right corner), reaching a more persistent R1/R2 structure. The effect is not as pronounced in the southern polar cap, though the farther location of the CGM pole still caused the orbit to reach the dusk meridian.

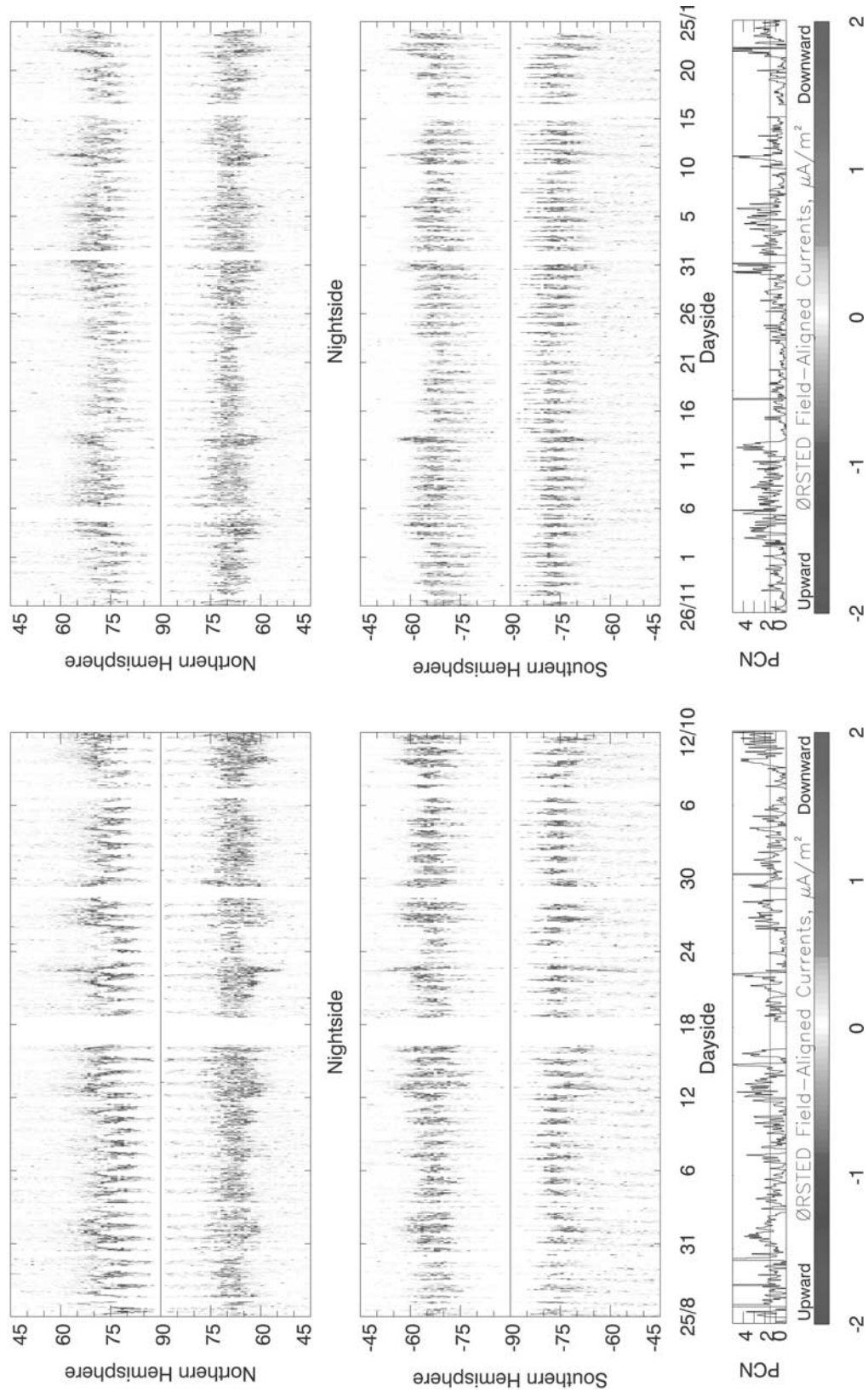

Figure 4. Field-aligned currents detected by Ørsted in the noon-midnight sector of the northern and southern polar caps. For each available pass the currents are plotted at the appropriate CGM latitude (vertical axis) against the day and month of 1999/2000 (horizontal axis). There are 14–15 passes/day. Downward currents are marked red/yellow, and upward currents are marked blue. (left) Equinox; (right) northern winter and southern summer. The northern polar cap magnetic activity index is shown in order to distinguish between quiet (PCN < 1.5) and disturbed (PCN > 1.5) conditions. See color version of this figure at back of this issue.

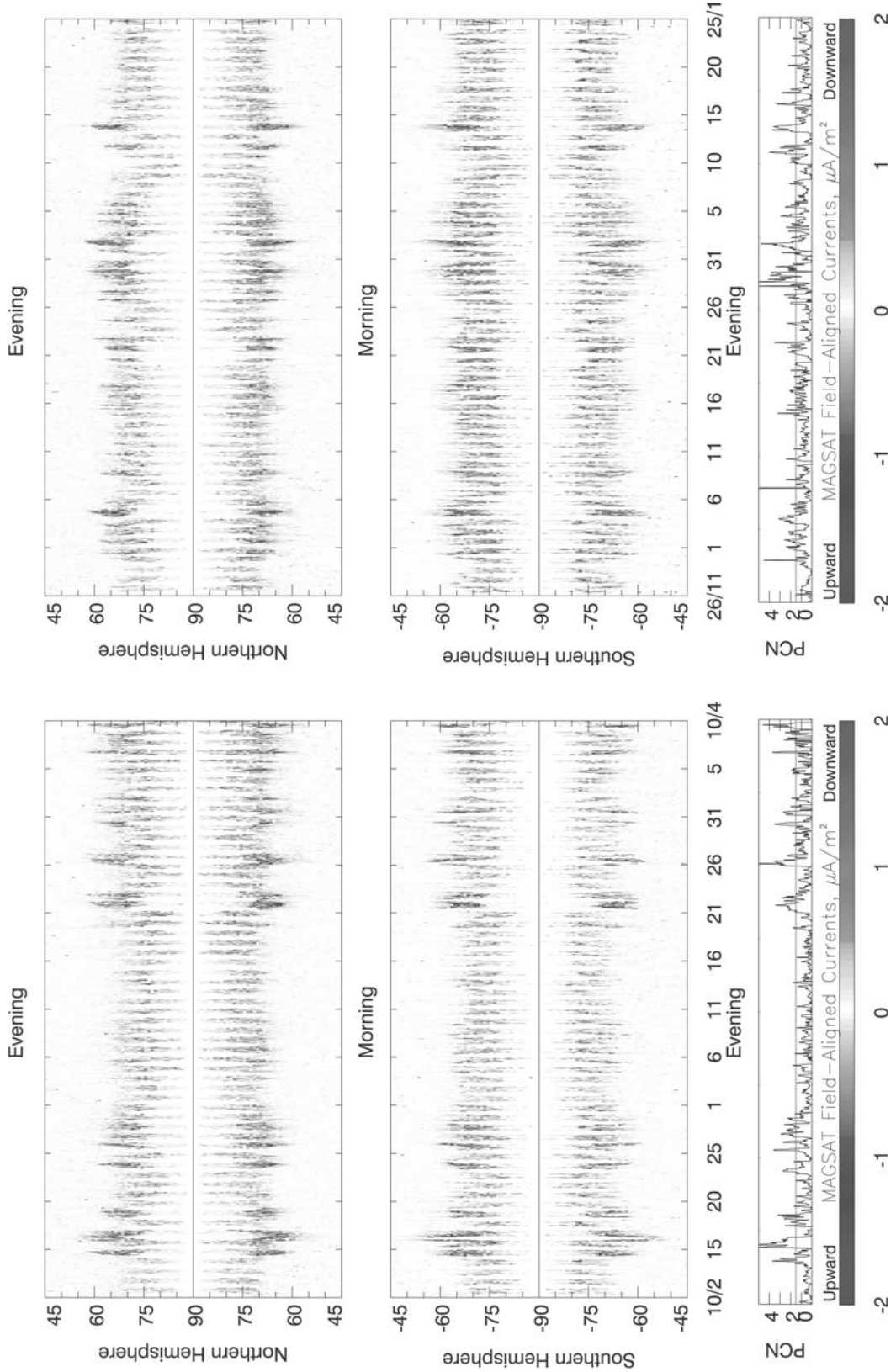

Figure 5. Field-aligned currents detected by Magsat in the dawn-dusk sector. The format is the same as for Figure 4. There are 15–16 passes/day. Downward currents are marked red/yellow, and upward currents are marked blue. (left) equinox; (right) northern winter and southern summer. See color version of this figure at back of this issue.

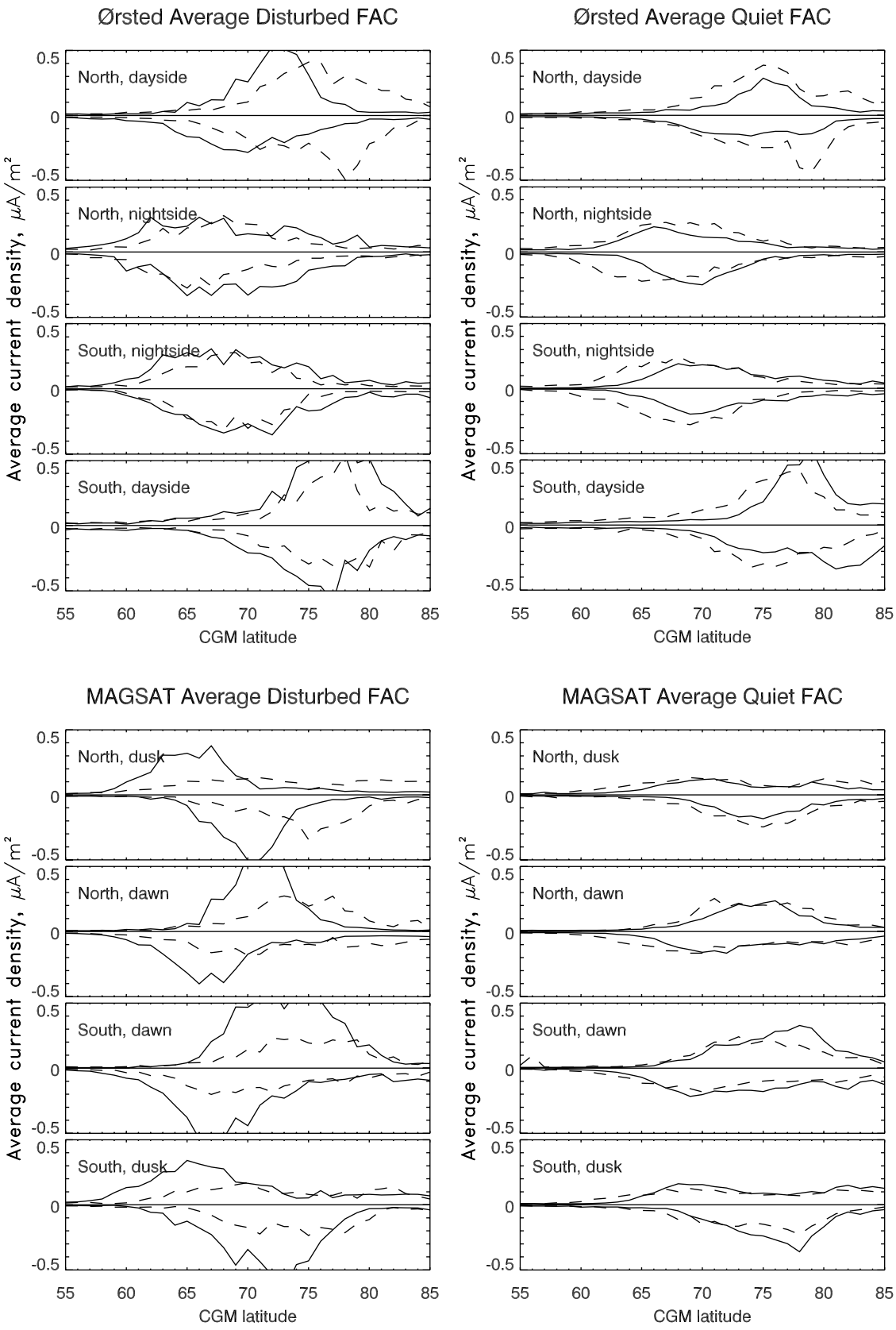

Figure 6. Field-aligned current densities versus CGM latitude averaged over the periods of Figures 4 and 5 for quiet (PCN < 1.5) and disturbed (PCN > 1.5) conditions. Positive (downward) and negative (upward) currents have been averaged separately. Solid lines show the results for northern winter/southern summer, and dashed lines show the results for equinox.

Table 1. Average Parameters of Field-Aligned Currents Inferred From Ørstead Observations[a]

			Dayside				Nightside			
Season	Hemisphere	FAC	Range, deg	P, deg	$j_{\|\|}$, μA/m^2	$J_{\|\|}$, A/m	Range, deg	P, deg	$j_{\|\|}$, μA/m^2	$j_{\|\|}$, μA/m
					Quiet Geomagnetic Conditions					
Equinox	North	Down	69–83	75.9±1.6	0.23±0.05	0.48±0.11	63–76	68.7±0.7	0.18±0.04	0.37±0.09
		Up	69–81	75.8±1.0	−0.24±0.06	−0.46±0.11	61–72	66.4±0.7	−0.18±0.04	−0.37±0.09
		Net			−0.01±0.04	0.02±0.06			0.00±0.02	0.00±0.03
	South	Down	70–82	76.3±0.6	0.24±0.06	0.49±0.10	63–73	68.1±0.6	0.18±0.05	0.35±0.10
		Up	70–82	76.0±1.0	−0.22±0.03	−0.44±0.07	63–73	68.4±0.4	−0.21±0.06	−0.37±0.12
		Net			0.02±0.03	0.05±0.06			−0.03±0.02	−0.02±0.03
Winter	North	Down	73–78	75.4±0.4	0.21±0.05	0.25±0.05	64–72	67.7±0.3	0.14±0.03	0.25±0.04
		Up	69–80	74.5±0.6	−0.13±0.03	−0.25±0.05	66–73	69.4±0.4	−0.19±0.03	−0.27±0.04
		Net			0.08±0.04	0.00±0.03			−0.05±0.02	−0.02±0.02
Summer	South	Down	74–85	79.1±1.0	0.28±0.05	0.48±0.07	66–74	69.9±0.5	0.16±0.03	0.28±0.06
		Up	72–85	79.1±0.6	−0.23±0.04	−0.44±0.07	67–74	70.3±0.3	−0.15±0.04	−0.26±0.06
		Net			0.05±0.04	0.04±0.06			0.01±0.03	0.02±0.04
					Disturbed Geomagnetic Conditions					
Equinox	North	Down	70–84	76.4±1.0	0.25±0.03	0.51±0.04	63–74	67.9±0.6	0.19±0.00	0.35±0.01
		Up	68–81	75.3±0.5	−0.25±0.00	−0.51±0.02	61–73	66.3±0.5	−0.17±0.01	−0.35±0.03
		Net			−0.01±0.03	0.00±0.02			0.02±0.01	0.01±0.02
	South	Down	72–83	77.1±0.6	0.24±0.04	0.46±0.08	63–73	68.1±0.9	0.19±0.01	0.34±0.03
		Up	71–82	76.8±1.2	−0.23±0.08	−0.41±0.10	64–74	68.9±0.8	−0.23±0.01	−0.38±0.02
		Net			0.01±0.05	0.05±0.06			−0.04±0.01	−0.04±0.03
Winter	North	Down	67–76	72.1±0.4	0.31±0.03	0.45±0.06	60–79	68.1±1.1	0.17±0.03	0.45±0.06
		Up	64–76	69.8±0.7	−0.19±0.01	−0.38±0.03	60–78	69.0±0.9	−0.22±0.02	−0.52±0.06
		Net			0.12±0.03	0.07±0.04			−0.04±0.01	−0.06±0.02
Summer	South	Down	68–85	76.8±0.9	0.34±0.05	0.73±0.10	62–77	68.4±0.7	0.22±0.04	0.48±0.09
		Up	68–83	75.1±0.6	−0.28±0.06	−0.59±0.11	62–77	69.3±0.5	−0.23±0.04	−0.51±0.09
		Net			0.06±0.01	0.13±0.03			0.01±0.03	−0.03±0.05

[a] The range is the extent in CGM latitudes where the average currents are > 0.1 μA/m^2, P is the average position of the FACs, and $j_{\|\|}$ the average density within the range. $J_{\|\|}$ is the current linear density integrated along the orbit from the lowest (55°) to the highest (85°) CGM latitudes. The first four rows correspond to the dashed line of the upper right plot of Figure 6, the next four rows correspond to the solid lines, and the last eight rows correspond equivalently to the upper left plot. The uncertainties on P, $j_{\|\|}$, and $J_{\|\|}$ are computed as rms deviations on subsets containing 35–40 polar passes.

[30] For the dawn/dusk observations of Magsat the R1/R2 structure is clearly seen, whereas the average positions given in Table 2 are to some extent contaminated by the existence of Region 0 currents. The Region 1 system is found ∼5° poleward of Region 2, as expected.

4.4. Current Densities

[31] The current densities listed in Tables 1 and 2 are smaller than what is typically seen in the literature owing to our choice of methods. Where, for example, *Fujii et al.* [1981] compute only the current density when identifiable current sheets exist, we are averaging over periods where the current systems are changing position.

[32] Figure 6 shows that the combined upward/downward current densities during quiet conditions typically are in the range 0.30–0.35 μA/m^2 for all cases except the dayside currents in the summer and equinox polar caps, where a significant intensification to ∼0.5 μA/m^2 is seen. The dayside currents during winter are of the same intensity as the nightside currents. In the dawn/dusk cases (e.g., Table 2) we find that during quiet (disturbed) conditions the current densities of Region 1 are stronger than those of Region 2 by ∼40% (∼50%); these ratios are slightly higher than the ones obtained by *Fujii et al.* [1981].

4.5. Total Currents

[33] Integrating the current densities for each of the curves in Figure 6, one may compare the average total upward and downward currents (in A/m). For the dawn/dusk currents we find that the Region 1 currents are generally stronger than the Region 2 currents, though the effect is not very pronounced during quiet conditions where the R1 currents on average exceeds the R2 currents by only 0.02 A/m. Disturbed conditions yield a stronger imbalance, particularly in the winter and summer seasons. On the dayside we most often find a total downward current greater than the upward current, whereas on the nightside the upward current is stronger.

4.6. Stability

[34] In order to check the stability of our results over the periods of observation, we have divided our data into subsets of 35–40 polar passes (in order to get a full sampling of the polar regions within each subset). This gives 4–5 subsets for disturbed conditions and 16–19 subsets for quiet conditions (12 for Ørsted at equinox). Computing the average positions of the FACs and the current densities for each subset, we obtain rms deviations for these quantities. The results are given in Tables 1 and 2. The rms deviations on the average positions are mostly in the range 0.5°–1.0°, with a few higher values, particularly for the R2 currents. The rms deviations on $j_{\|\|}$ are mostly below 0.1 μA/m^2 and on $J_{\|\|}$ are mostly below 0.1 A/m, both values significantly below the values of these quantities themselves.

5. Discussion

[35] Defining the size of the polar cap by estimating the over-the-pole distance between the average positions of the dawn-dusk and dayside-nightside field-aligned currents, we conclude from the Magsat data that the "dawn-to-dusk" size of the polar cap in both the Northern and Southern Hemispheres is ∼34° in average independent of season. Ørsted observations show that the "day-to-night" size of the polar cap is stable over winter and equinox and is 36°–37°. Though the average nightside FAC system moves slightly poleward from equinox to winter, this is balanced by a movement equatorward of the dayside currents. That day-to-night distance decreases significantly in the summer polar cap with both dayside and nightside currents moving poleward to a distance of ∼32°.

Table 2. Average Parameters of Field-Aligned Currents Inferred From Magsat Observations[a]

			Dawn				Dusk			
Season	Hemisphere	FAC	Range, deg	P, deg	$j_\parallel$, μA/m^2	$J_\parallel$, A/m	Range, deg	P, deg	$j_\parallel$, μA/m^2	$J_\parallel$, μA/m
					Quiet Geomagnetic Conditions					
Equinox	North	R1	69–80	74.4±1.0	0.19±0.05	0.34±0.09	70–79	74.7±0.9	−0.19±0.05	−0.33±0.09
		R2	65–82	70.4±1.3	−0.13±0.04	−0.31±0.09	67–83	73.3±1.0	0.12±0.03	0.28±0.08
		Net			0.06±0.03	0.03±0.04			−0.07±0.03	−0.04±0.03
	South	R1	70–80	74.8±0.8	0.18±0.06	0.34±0.08	68–80	74.9±1.1	−0.16±0.04	−0.30±0.07
		R2	65–81	71.0±1.3	−0.13±0.04	−0.32±0.08	67–84	74.9±1.8	0.11±0.02	0.28±0.07
		Net			0.05±0.03	0.02±0.04			−0.05±0.03	−0.02±0.02
Winter	North	R1	71–79	74.9±0.4	0.18±0.03	0.27±0.05	72–78	74.9±0.4	−0.15±0.02	−0.21±0.02
		R2	68–78	71.6±0.2	−0.13±0.03	−0.25±0.05	69–71	70.0±0.1	0.12±0.03	0.20±0.03
		Net			0.04±0.02	0.02±0.02			−0.04±0.01	−0.01±0.02
Summer	South	R1	70–82	76.3±0.6	0.21±0.04	0.39±0.07	70–80	75.6±0.6	−0.22±0.03	−0.37±0.06
		R2	66–85	74.4±1.4	−0.15±0.02	−0.39±0.05	67–85	75.4±1.1	0.14±0.02	0.31±0.04
		Net			0.06±0.04	0.00±0.06			−0.09±0.03	−0.06±0.04
					Disturbed Geomagnetic Conditions					
Equinox	North	R1	70–79	74.6±0.6	0.21±0.04	0.34±0.07	69–79	74.7±0.9	−0.19±0.04	−0.34±0.07
		R2	66–82	72.6±1.0	−0.13±0.02	−0.32±0.06	65–85	74.5±1.1	0.11±0.03	0.29±0.07
		Net			0.08±0.02	0.02±0.02			−0.08±0.04	−0.05±0.04
	South	R1	70–80	75.1±0.6	0.19±0.07	0.33±0.13	68–80	74.3±1.3	−0.17±0.06	−0.32±0.12
		R2	65–78	70.2±0.9	−0.16±0.06	−0.32±0.11	64–82	72.2±1.6	0.13±0.02	0.30±0.06
		Net			0.03±0.02	0.01±0.03			−0.04±0.02	−0.02±0.03
Winter	North	R1	67–75	71.0±0.2	0.40±0.04	0.50±0.04	66–74	70.0±0.2	−0.32±0.04	−0.42±0.04
		R2	61–71	66.4±0.3	−0.24±0.02	−0.43±0.03	61–70	65.4±0.4	0.24±0.04	0.37±0.04
		Net			0.16±0.03	0.07±0.03			−0.08±0.01	−0.04±0.01
Summer	South	R1	67–80	73.2±0.9	0.42±0.04	0.76±0.08	64–78	71.4±0.7	−0.33±0.01	−0.64±0.03
		R2	62–82	68.5±0.5	−0.29±0.03	−0.67±0.06	60–76	66.2±0.6	0.21±0.02	0.48±0.03
		Net			0.13±0.03	0.09±0.04			−0.21±0.01	−0.16±0.02

[a] The format is the same as that of Table 1. The first four rows correspond to the dashed lines of the lower right plot of Figure 6, the next four rows correspond to the solid lines, and the last eight rows correspond to the lower left plot.

[36] This establishes the general shape and seasonal dependence of the global field-aligned current systems: the ionospheric footprint of the global FAC system is oval-like in shape with a "fixed" (on average) dawn-dusk distance of 34° (∼3800 km), while the day-night distance changes from 36°–37° (4000–4100 km) during winter and equinox to 32° (∼3550 km) during summer. This result is consistent with conclusions previously obtained [*Fujii et al.*, 1981] from TRIAD satellite data that the dayside field-aligned currents are found at 1°–3° higher latitudes in the summer hemisphere in comparison to the winter hemisphere. From Ørsted data we conclude also that the nightside currents move poleward in the summer polar cap.

[37] We have also computed estimates of the average FACs over both polar caps and during different seasons. For example, from Table 2 one can see that during equinox all currents are well balanced for both the quiet and disturbed conditions. However, if we average the "quiet" R1 current densities at dawn and dusk during all seasons, we obtain ∼0.19 μA/m^2, which is ∼1.5 times larger than the corresponding R2 average (∼0.13 μA/m^2). For disturbed conditions these densities do not change much during equinox; however, maintaining the same ratio, they double during winter and summer.

[38] Nevertheless, the average current intensities (in A/m) are generally well balanced between Regions 1 and 2 in both the dawn and dusk MLT sectors during all seasons. Holding a hypothesis of a single current source in the magnetosphere, we expect that the currents flowing into the summer polar cap should be of a larger intensity than the currents supplied to the winter polar cap. *Fujii et al.* [1981] obtained that the R1/R2 current intensities in the dayside portion of the polar cap "are larger during the summer (in comparison to winter) by a factor of about 2" (p. 1103). In our analysis we confirm these results, though our estimates from Table 2 show the summer/winter ratio to be only ∼1.5 times during both the quiet and disturbed conditions.

[39] Unlike the results obtained by *Fujii and Iijima* [1987], Table 2 does not show an increase in net currents in the sunlit polar cap during quiet conditions. However, considerable net currents are seen for disturbed conditions during winter as well as during summer. These currents are either balanced or even larger in the dusk sector; however, *Fujii et al.* [1994, Table 1] noted that during substorms there appear to be considerable net currents in the dawn and nighttime sector but little net current in the dusk sector. We note that because *Fujii et al.* [1994] have dealt with currents in the shaded region (comparing to auroral configurations), the latter comparison should better be done with the nightside currents in winter during disturbed conditions in our Table 1. Thus we conclude that the obtained balance between the corresponding pairs of R1(↓↑) and R2(↑↓) currents at either side of the polar cap, as well as the R1/R2 balance at dawn and dusk, justifies the FAC closure through the meridional currents in the ionosphere.

[40] The dayside and nightside FAC systems should be interhemispherically coupled either through the dayside magnetopause and magnetospheric mantle or through the nightside, substorm-related connection to the magnetospheric plasma sheet. Therefore, though we organized our tables similarly, we should keep in mind that the downward/upward FACs at the dayside and nightside should also be balanced between hemispheres. However, as seen in Figure 1 (top plots), we should admit that our analysis of these currents during winter/summer seasons could be slightly "contaminated" by the dayside Region 0 currents. Nevertheless, the numbers in Table 1 show clearly that almost all pairs of the downward/upward FACs at the dayside and nightside are well balanced during all seasons for quiet conditions. During disturbed conditions, one can see that the northern equinox FACs are well balanced because there is almost no "contamination" from the R0 currents; however, larger net currents in all other situations indicate that the FAC imbalance likely was caused by the effects from R1/R2 currents, similar to those analyzed in Table 2 from Magsat data.

[41] As noted by *Fujii et al.* [1981], our analysis (see Table 1) shows that the dayside FACs during summer are larger by a factor of ~1.8 in comparison to winter during quiet conditions; this ratio decreases to ~1.6 for disturbed conditions. At the same time, Table 2 shows that the summer/winter FAC ratio is persistent at dawn and dusk, amounting to ~1.5 for both the quiet and disturbed conditions. During equinox the interhemispheric FAC ratio (e.g., southern/northern or vice versa) equals exactly 1.0 everywhere at all MLT sectors. This can be explained by the significant increase in the polar cap conductivity Σ_{si} caused by solar illumination, while the conductivity Σ_{pp} produced by the particles precipitation (i.e., during disturbed conditions) is less important during summer because the resulting conductivity Σ is proportional to the corresponding ionization functions: $\Sigma = (\Sigma_{si}^2 + \Sigma_{pp}^2)^{1/2}$.

[42] For example, let us assume that only the background particle precipitation produces any conductivity in the winter polar cap and the "quiet conditions" summer/winter ratio is 1.8 (that is, $\Sigma_{si}^{sum} = 1.8\ \Sigma_{pp}^{win}$). Then let us add $\Sigma_{pp}^{disturb} \sim \Sigma_{pp}^{win}$ to both the summer and winter background conductivities; this will decrease the "disturbed conditions" summer/winter ratio to ~1.5. The latter number is close to our estimates for the dayside FACs in Table 1, but we note that our experimental nighttime summer/winter ratio equals exactly 1.0. However, *Newell et al.* [2001] show in their review that intense aurora (caused by particle precipitation) are suppressed in sunlight as compared with darkness with the 3:1 ratio. Therefore, in the example above we should add one third of $\Sigma_{pp}^{disturb}$ to the summer conductivity (but the full value to the winter conductivity); that will bring the "disturbed conditions" summer/winter ratio down to ~1.3. The latter number is closer to our experimental nightside summer/winter ratio of 1.0, which suggests that the magnetosphere-ionosphere system drives the nightside FACs symmetrically through the two hemispheres. Thus we conclude that the nightside currents are maintained at the same intensity during summer, winter, and equinox for both the quiet and disturbed conditions in both hemispheres, indicating no increases from winter to summer.

6. Summary and Conclusions

[43] The seasonal effect on spatial configurations of both the R1/R2 and dayside/nightside FAC systems is analyzed in this study. It is shown that the dawn/dusk projections of the R1/R2 system to the ionosphere are separated "over-the-pole" by ~34°, and this distance is stable through all seasons. The corresponding distance between the dayside and nightside FACs increases from 32° during summer to 37° during equinox and winter. The decrease in the size of summer polar cap is caused by a shift of both daytime and nighttime currents to higher magnetic latitudes.

[44] Our results suggest that the R1/R2 and dayside field-aligned currents are well balanced between the pairs of downward/upward currents for all seasons as well as between hemispheres during equinox. We were not able to confirm results reported by *Fujii and Iijima* [1987] and *Fujii et al.* [1994] that the net currents tend to increase with an enhancement of ionospheric conductivity caused by the solar illumination or substorm activity.

[45] Thus we believe that the results obtained in this study provide the solid confirmation of existing seasonal dependence in the global field-aligned current system generated and maintained by the "directly loading" solar wind-magnetosphere interaction, which controls the follow-on "directly driven" magnetosphere-ionosphere coupling processes. This generator produces FACs from various interaction processes, such as the quasi-viscous interaction of the solar wind plasma with the Earth's magnetosphere and reconnection of the IMF B_z and B_y components with the geomagnetic field at the subsolar magnetopause. We believe that during equinox this source should supply field-aligned currents of the same intensity to both the northern and southern polar caps; this is confirmed in Tables 1 and 2 for the quiet geomagnetic activity.

[46] However, as shown in Tables 1 and 2, the FAC intensities are larger by a factor of 1.5–1.8 in the dayside sunlit (summer) polar cap in comparison to the winter hemisphere; at the same time, the nightside currents indicate no increases from winter to summer. Suppression of intense aurora in the sunlit polar cap works in favor of the latter result. The significant difference between the dayside, dawn, and dusk FACs between summer and winter hemispheres may be explained by an ionospheric resistivity "load": in darkness the ionospheric conductivity is low, and therefore there are almost no Pedersen currents to close the dawn-dusk R1 and dayside field-aligned currents; the closure may only occur at the ionospheric *F* layer altitudes through the Alfvén waves.

[47] We also want to note that 20 years separate observations from the two satellites and both Magsat and Ørsted were flown during solar maximums. The latter does not allow us to estimate correctly if there is any influence on the FAC distributions from the solar activity cycle.

[48] **Acknowledgments.** We are grateful for the support of the Ørsted Project Office and the Ørsted Science Data Center at the Danish Meteorological Institute. The Ørsted Project is funded by the Danish Ministry of Transport, Ministry of Research and Information Technology, and Ministry of Trade and Industry. Additional support was provided by the U.S. National Aeronautics and Space Administration (NASA), European Space Agency (ESA), Centre Nationale d'Etudes Spatiales (CNES, France) and Deutsche Agentur für Raumfahrtangelegenheiten (DARA, Germany). We also thank the NASA National Space Science Data Center for providing Magsat data on a CD-ROM. V.O.P. acknowledges support from the NSF awards OPP-9614175 and ATM-9727554 to the University of Michigan.

[49] Michel Blanc thanks Ryoichi Fujii and Alan Rodger for their assistance in evaluating this paper.

References

Carlson, C. W., et al., FAST observations in the downward auroral current region: Energetic upgoing electron beams, parallel potential drops, and ion heating, *Geophys. Res. Lett.*, *25*, 2017, 1998.

Elphic, R. C., et al., The auroral current circuit and field-aligned currents observed by FAST, *Geophys. Res. Lett.*, *25*, 2033, 1998.

Erlandson, R. E., L. J. Zanetti, T. A. Potemra, and P. F. Bythrow, IMF B_y dependence of Region 1 Birkeland currents near noon, *J. Geophys. Res.*, *93*, 9804, 1988.

Fujii, R., and T. Iijima, Control of ionospheric conductivities on large-scale Birkeland current intensities under geomagnetic quiet conditions, *J. Geophys. Res.*, *92*, 4505, 1987.

Fujii, R., T. Iijima, T. A. Potemra, and M. Sugiura, Seasonal dependence of large-scale Birkeland currents, *Geophys. Res. Lett.*, *8*, 1103, 1981.

Fujii, R., R. A. Hoffman, P. C. Anderson, J. D. Craven, M. Sugiura, L. A. Frank, and N. C. Maynard, Electrodynamic parameters in the nighttime sector during auroral substorms, *J. Geophys. Res.*, *99*, 6093, 1994.

Gustafsson, G., N. E. Papitashvili, and V. O. Papitashvili, A revised corrected geomagnetic coordinate system for Epochs 1985 and 1990, *J. Atmos. Terr. Phys.*, *54*(11/12), 1609, 1992.

Hoffman, R. A., R. Fujii, and M. Sugiura, Characteristics of the field-aligned current system in the nighttime sector during auroral substorms, *J. Geophys. Res.*, *99*, 21,303, 1994.

Iijima, T., and T. A. Potemra, The amplitude distribution of field-aligned currents at northern high latitudes observed by Triad, *J. Geophys. Res.*, *81*, 2165, 1976.

Iijima, T., and T. Shibaji, Global characteristics of northward IMF-associated (NBZ) field-aligned currents, *J. Geophys. Res.*, *92*, 2408, 1987.

Iijima, T., T. A. Potemra, L. J. Zanetti, and P. F. Bythrow, Large-scale Birkeland currents in the dayside polar region during strongly northward IMF: A new Birkeland current system, *J. Geophys. Res.*, *89*, 7441, 1984.

Langel, R. A., and R. H. Estes, The near-earth magnetic field at 1980 determined from Magsat data, *J. Geophys. Res.*, *90*, 2495, 1985.

Neubert, T., M. Mandea, G. Hulot, R. von Frese, F. Primdahl, J. L. Jørgensen, E. Friis-Christensen, P. Stauning, N. Olsen, and T. Risbo, Ørsted satellite captures high-precision geomagnetic field data, *Eos Trans. AGU*, *82*(7), 81, 2001.

Newell, P. T., C.-I. Meng, and S. Wing, Relation to solar activity of intense aurorae in sunlight and darkness, *Nature*, *393*, 342, 1998.

Newell, P. T., R. A. Greenwald, and J. M. Ruohoniemi, The role of the ionosphere in aurora and space weather, *Rev. Geophys.*, *39*, 137, 2001.

Olsen, N., T. J. Sabaka, and L. Tøffner-Clausen, Determination of the IGRF 2000 model, *Earth Planets Space*, *52*(12), 1175, 2000a.

Olsen, N., et al., Ørsted Initial Field Model, *Geophy. Res. Lett.*, *27*, 3606, 2000b.

Papitashvili, V. O., B. A. Belov, D. S. Faermark, Y. I. Feldstein, S. A. Golyshev, L. I. Gromova, and A. E. Levitin, Electric potential patterns in the northern and southern polar regions parameterized by the interplanetary magnetic field, *J. Geophys. Res.*, *99*, 13,251, 1994.

Papitashvili, V. O., F. Christiansen, and T. Neubert, Field-aligned currents during IMF $\sim$ 0, *Geophys. Res. Lett.*, *28*(15), 3055–3058, 2001.

Potemra, T. A., L. J. Zanetti, P. F. Bythrow, and A. T. Y. Lui, B_y-dependent convection patterns during northward interplanetary magnetic field, *J. Geophys. Res.*, *89*, 9753, 1984.

Troshichev, O. A., A. L. Kotikov, E. M. Shishkina, V. O. Papitashvili, C. R. Clauer, and E. Friis-Christensen, DPY currents in the cusp/cleft region: A crucial role of southward interplanetary magnetic field, *J. Geophys. Res.*, *102*, 4777, 1997.

Vassiliadis, D., V. Angelopoulos, D. N. Baker, and A. J. Klimas, The relation between the northern polar cap and auroral electrojet geomagnetic indices in the wintertime, *Geophys. Res. Lett.*, *23*, 2781, 1996.

Watanabe, M., T. Iijima, M. Nakagawa, T. A. Potemra, L. J. Zanetti, S. Ohtani, and P. T. Newell, Field-aligned current systems in the magnetospheric ground state, *J. Geophys. Res.*, *103*, 6853, 1998.

Yamamoto, T., S. Inoue, and M. Ozaki, On the limitation of the current sheet approximation in estimation of the northward B_z associated field-aligned currents, *J. Geophys. Res.*, *105*, 21,143, 2000.

Zanetti, L. J., W. Baumjohann, and T. A. Potemra, Ionospheric and Birkeland current distributions inferred from the MAGSAT magnetometer data, *J. Geophys. Res.*, *88*, 4875, 1983.

Zmuda, A. J., and J. C. Armstrong, The diurnal flow pattern of field-aligned currents, *J. Geophys. Res.*, *79*, 4611, 1974.

F. Christiansen and V. O. Papitashvili, Solar-Terrestrial Physics Division, Danish Meteorological Institute, Lyngbyvej 100, DK-2100 Copenhagen, Denmark. (fch@dmi.dk; vp@dmi.dk)

T. Neubert, Danish Space Research Institute, Juliane Maries Vej 30, DK-2100 Copenhagen, Denmark. (neubert@dsri.dk)

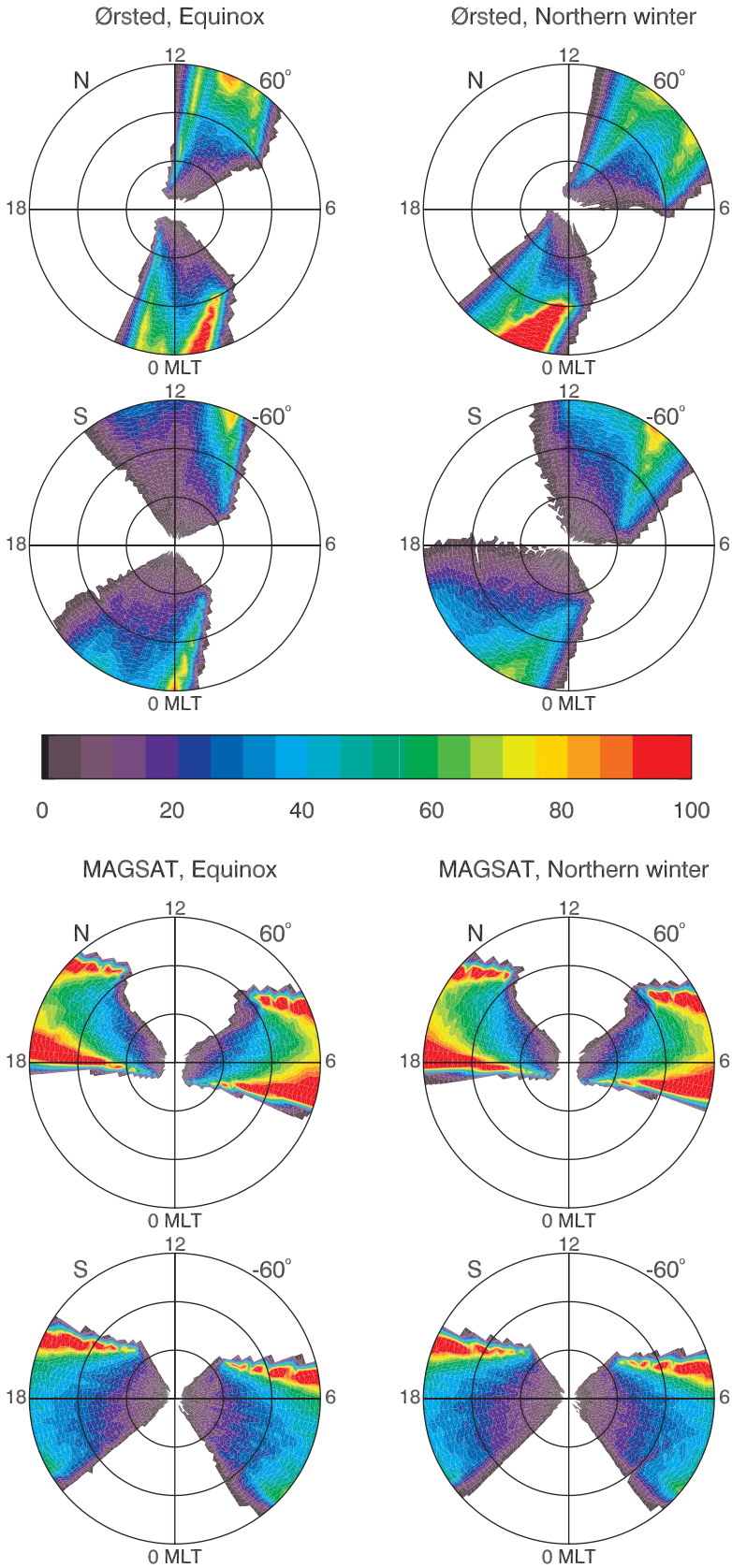

Figure 1. Data coverage for Ørsted and Magsat in the CGM latitude-MLT coordinates. Red/yellow areas denote strong data coverage; purple/blue areas denote weak data coverage. The numbers on the color bar refer to the number of current density measurements in bins of 1° magnetic latitude and 20 min MLT. The data have been discarded where the satellites' orbits were passing the CGM latitudes at an angle below 45°. This in combination with the diurnal variation of the magnetic coordinate system relative to the satellite's orbit determines the data coverage.

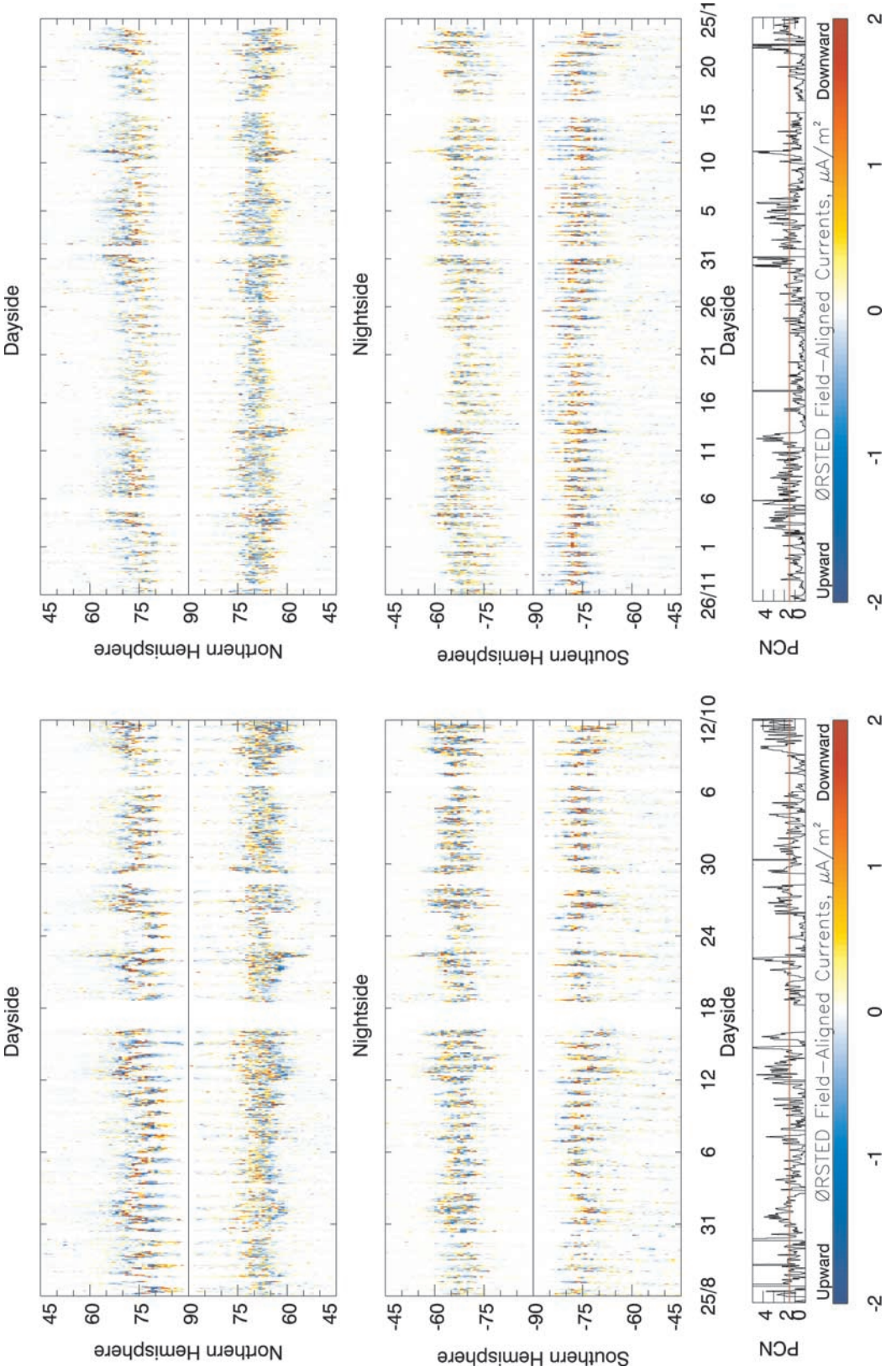

Figure 4. Field-aligned currents detected by Ørsted in the noon-midnight sector of the northern and southern polar caps. For each available pass the currents are plotted at the appropriate CGM latitude (vertical axis) against the day and month of 1999/2000 (horizontal axis). There are 14–15 passes/day. Downward currents are marked red/yellow, and upward currents are marked blue. (left) Equinox; (right) northern winter and southern summer. The northern polar cap magnetic activity index is shown in order to distinguish between quiet (PCN < 1.5) and disturbed (PCN > 1.5) onditions.

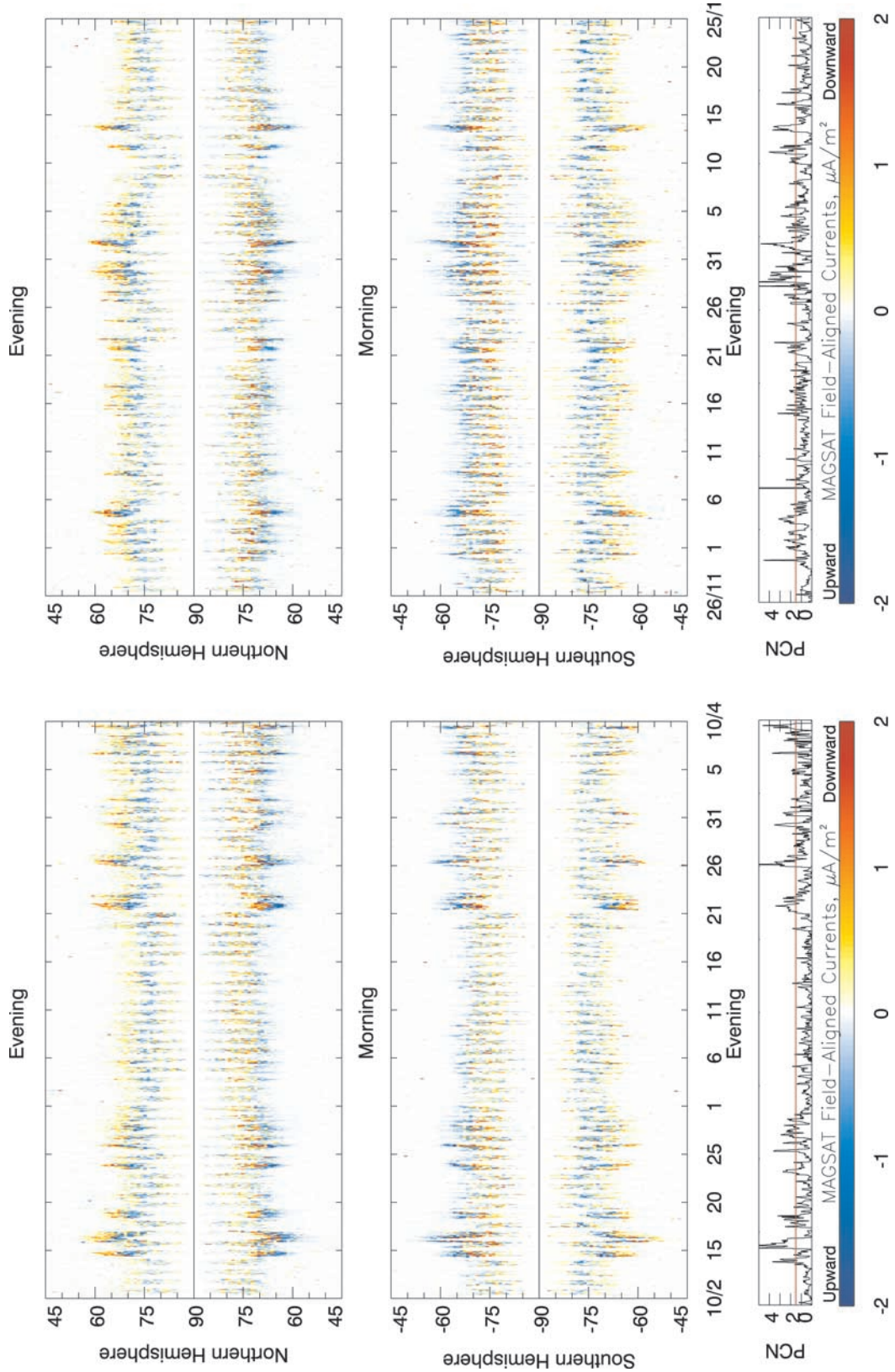

Figure 5. Field-aligned currents detected by Magsat in the dawn-dusk sector. The format is the same as for Figure 4. There are 15–16 passes/day. Downward currents are marked red/yellow, and upward currents are marked blue. (left) equinox; (right) northern winter and southern summer.